Model Reduction of Turbocharged (TC) Spark Ignition (SI) Engine

Abstract

In this paper, we propose a new procedure to reduce the order of control oriented TC SI engine models. The techniques is based on the identification of time scale separation within the dynamics of various engine state variables with pertinent use of the perturbation theory. The model reduction is accomplished in two steps and exploits the dynamic and physical characteristics of engine design and its operation. In the first step, regular and singular perturbation theories are collectively employed to eliminate temperature dynamics and replace them with their quasi-steady state values. This is followed by the elimination of fast pressures. As a result, a library of engine models is obtained which are associated with each other on sound theoretical basis. Different assumptions under which this modeling is realizable are presented and their existence in the context of engine is discussed. The limitations of the proposed engine model as a true representation of the actual engine behavior (as depicted by the comprehensive model) are qualitatively assessed through comprehensive simulation studies.

1 Introduction

With the automotive industry growing and its market maturing, emission and fuel economy standards are becoming increasingly stringent. While minimizing emissions and improving fuel economy, it is also of a paramount importance from the customers' point of view that there is a minimal (or no) sacrifice in terms of the drivability. Developing such an engine control system which delivers these conflicting requirements in a most efficient way has been a major challenge, especially during the last three to four decades.

Obtainment of best possible engine performance with minimum possible emission calls for the implementation of much improved control methods and hardware. Here, the development and reduction of mathematical models of the engine becomes quite crucial as most of the existing advanced control methodologies require the knowledge of the mathematical model of the plant and that too in a sufficiently simplified form.

Among the existing approaches for engine modeling, a major trend has been to use the measured engine data to establish functional relationships between inputs and outputs to obtain steady state engine maps. Such approaches, though widely used, yield models that are engine specific, leading to a lack of generalization capability in the model itself, and any engine components parts (such as engine controllers) that may be based upon it. Moreover, heavy dependence on the look-up tables is often undesirable as the accuracy is highly dependent on the amount of data available, extrapolation is unreliable and may induce unnecessary numerical noise (discontinuities) [7]. This is a major limitation of the empirical, quasi-static approach.

An alternative is to formulate a physics-based mathematical model of the system.

This model should accurately evince all the fundamental phenomena associated with the engine operation so that tasks of perturbation studies, sensitivity and error analysis and controller design can be readily carried out. An important class of engine models established on physical laws, which over the past three decades have proven to be quite effective in performing studies on engine dynamics, engine supervision and development of advanced engine control, is the mean value engine models (MVEM) [6],[7]. MVEMs describe the average engine behavior over several engine event cycles. For *naturally aspirated* engines, such model have now been well researched and are being successfully utilized in several aspects of engine operation including its control, torque management and supervision [8].

Furthermore, in order to regulate emissions in naturally aspirated SI engines, the use of three way catalytic converter has thus far been deemed quite effective which converts the harmful byproducts of combustion process into less harmful products like CO_2 and water vapors. However, in recent times there has been a further push to reduce the CO_2 emissions as it is a key element in causing global warming due to green house effect. One proven way to reduce CO_2 emissions is to reduce the size of the engine cylinders [18], [4]. This, however, comes at the expense of maximum torque that the engine can generate and hence affects drivability. One surest way to generate more power out of the engine of given volume is to increase the amount of air and fuel that it can burn by packing more air and fuel. A turbocharger does exactly that by compressing the incoming air to a pressure higher than that of the ambient and as a result deliver greater charge densities with the lower pumping losses associated with reduced capacity engine.

Due to the proven efficacy of the MVEM of naturally aspirated engines in control

related implementations, efforts have been directed in obtaining similar models for TC SI engines as well. Initial endeavours in this direction include [14] and [16] whereby the problem of control oriented modeling of the turbocharger is considered. In particular, [14] compares and discusses three key turbine and compressor MVEM models as described in [11], [15] and [17]. These works are followed by [4] where a fully validated comprehensive 13^{th} order TC SI engine model is developed. The modeling strategy is to first consider the physics of engine components (like air filter, compressor, intercooler, throttle, engine, turbine and exhaust system) which yields model structures as they behave in the engine setting. The resulting componentwise engine model is used by the same authors for further investigation with regard to cylinder air charge estimation and engine control and optimization ([2], [3]).

Nevertheless, none of the above referred papers utilize the dynamic and physical attributes of the engine to develop a systematic procedure for model reduction. A rigorous procedure to build such reduced order models will improve portability of the engine models, leading to reduced engine calibration times as prior work in controller development on one turbocharged system can be utilized on multiple systems. Moreover, implementation of advanced nonlinear and robust design tools, which so far have not been practiced (apart from [10] in the context of diesel engines) entails the system models to be sufficiently simple. The existing reduced order TC SI engine models (see [13] for example) are strictly based on empirical findings and are valid only in a very narrow range of operation which make them inappropriate for representing other engines.

In this contribution we propose a systematic procedure to develop a set of new reduced order but versatile mean value models for turbocharged SI engines. The aim

here is to simplify and reduce the order of a comprehensive higher order engine model (as described in [1] and [4]) without compromising the physics involved in their development. The order reduction is accomplished by the identification of multiple time scale separation within the dynamics of temperatures and pressures corresponding to various engine compartments and hence singular perturbation theory is applicable. Different sets of assumptions under which these model reductions are applicable are presented and discussed. As a result, a library of three engine models is obtained. It is shown that all the models evince similar characteristics under a wide range of operating conditions provided certain sets of mild assumptions hold.

The advantages of reduced order models thus obtained are that they are highly suited for development of enhanced control methods, are appropriate for analyzing the system behavior by simulation studies and at the same time provide valuable insight into the engine operation. The validity of the assumptions in the context of actual existing engines is scrutinized first analytically and then verified with some simulation studies.

In section 2 below, the structure of 13^{th} order engine, as presented in [1], is briefly reviewed and summarized in the form of stage 1 model (Σ_1). Section 3 deals with the development of a procedure for model simplification by order reduction. This section is partitioned into subsections 3.1 and 3.2 which discuss two stages of model reduction and present the end results in the form of stage 2 (Σ_2) and stage 3 (Σ_3) models, respectively.

2 Stage 1 Engine Model

In this section, we briefly describe the comprehensive componentwise engine model introduced in [1] and [4]. This model incorporates the physics due to individual constituent components and their interactions through pipes and/or manifolds (referred to as *control volumes*), builds on previous work in the engine modeling and has been extensively validated. Therefore, this model represents state-of-the-art progress in control-oriented modeling of TC SI engines and we adopt it as our starting point. It is important to mention that the order of this model is too high which makes it unsuitable for design of highly sophisticated controllers. In rest of this section, we summarize its structure in the form of stage 1 model denoted by Σ_1.

2.1 Control Volumes

The modeling principle is to place *components* (like the air filter, compressor, intercooler, engine, turbine and turbo-shaft) between the control volumes. The pressure and temperature within the control volumes are determined by mass flow into and out of the volume. On the other hand, mass flows and temperatures of the flows at the inlet of control volumes are determined by the components on the basis of the pressure and temperature in the control volumes before and after them. In other words, behavior of the gas within the control volumes (CV) is dictated by filling and emptying dynamics of temperatures and pressures. In a TC SI engine, there are six control volumes that are modeled the same way. Each control volume is modeled as a dynamic element with two states, namely temperature $T_{cv}(t)$ and pressure $P_{cv}(t)$, taking into account mass and energy balances. The Table 1 lists all the control volumes and their corresponding

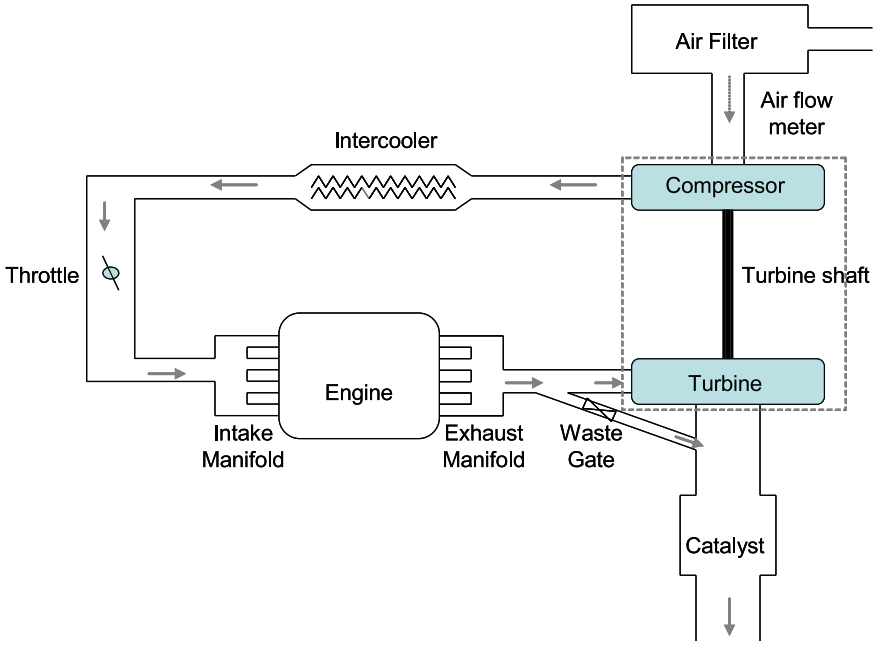

Figure 1: Schematic of TC SI Engine

state variables. The inputs, outputs and parameters corresponding to each control volume are listed in the Table 2. Figure 1 shows the block diagram representation of the TC SI engine as a cascade connection of various components that are connected via pipes (control volumes).

2.2 Equations

The equations describing the dynamics of pressure and temperature within the control volumes are derived from the laws of conservation of mass and energy. Specifically, the dynamic equation for temperature comes from differentiation of the law of conservation of energy, while the equation for pressure dynamics originates by differentiating the

Table 1: TC SI Engine Control Volumes

Control Volume (cv)	Variables
Air filter (af)	$P_{af}(t)$ (Pa), $T_{af}(t)$ (K)
Compressor (c)	$P_c(t)$ (Pa), $T_c(t)$ (K)
Intercooler (ic)	$P_{ic}(t)$ (Pa), $T_{ic}(t)$ (K)
Intake manifold (im)	$P_{im}(t)$ (Pa), $T_{im}(t)$ (K)
Exhaust manifold (em)	$P_{em}(t)$ (Pa), $T_{em}(t)$ (K)
Turbine (t)	$P_t(t)$ (Pa), $T_t(t)$ (K)

Table 2: Control volume inputs, outputs and parameters

Inputs	$\dot{m}_{cv_{in}}(t)$ (Kg/s), Mass flow in
	$\dot{m}_{cv_{out}}(t)$ (Kg/s), Mass flow out
	$T_{cv_{in}}(t)$ (K), Temperature upstream
Outputs	$P_{cv}(t)$ (Pa), Pressure in the control volume
	$T_{cv}(t)$ (K), Temperature in the control volume
Parameters	V_{cv} (m^3), Volume of the control volume
	R ($\frac{J}{KgK}$), Gas constant
	γ, ratio of specific heats $\frac{c_p}{c_v}$

ideal gas law [6].

$$\dot{P}_{cv}(t) = \left(\frac{\gamma R}{V}\right)\left[\dot{m}_{cv_{in}}(t)T_{cv_{in}}(t) - \dot{m}_{cv_{out}}(t)T_{cv}(t)\right] \quad (1)$$

$$\dot{T}_{cv}(t) = \left(\frac{T_{cv}(t)}{P_{cv}(t)}\right)\left(\frac{\gamma R}{V_{cv}}\right)\left[\dot{m}_{cv_{in}}(t)T_{cv_{in}}(t) - \dot{m}_{cv_{out}}(t)T_{cv}(t) - \frac{T_{cv}(t)}{\gamma}(\dot{m}_{cv_{in}}(t) - \dot{m}_{cv_{out}}(t))\right] \quad (2)$$

It may be noted that in equations (1)-(2), mass flows, $\dot{m}_{cv_{in}}(t)$ and $\dot{m}_{cv_{out}}(t)$, are functions of state variables, $P_{cv}(t)$ and $T_{cv}(t)$. However, for the sake of brevity the dependence of mass flows on $P_{cv}(t)$ and $T_{cv}(t)$ is omitted in the notations $m_{cv_{in}}(t)$ and $m_{cv_{out}}(t)$.

2.3 Stage 1 model

The following assumptions apply:

Assumption 1 No substantial heat or mass transfer through the control volume walls takes place.

Assumption 2 The temperature and pressure in whole control volume are uniform.

Assumption 3 The fluid is a perfect gas.

Remark 1: Assumption 1 may not hold strictly, as some heat transfer to the engine control volumes walls does occur. This assumption can be easily relaxed by including a term $\dot{Q}$ in the dynamical equations, (1) and (2), to account for this heat transfer. However, the rate of heat transfer is usually quite small in comparison to pressure and temperature dynamics and hence is dropped for notational convenience.

Remark 2: Assumption 2 ensures that no pulsating due to air resonance takes place. Though real engines do exhibit this phenomenon due to the sudden opening and closing of values, its speed is of the order of sound waves. While considering the mean value model this process can be ignored.

Remark 3: By assumption 3, we can apply ideal gas law which governs the dynamics of pressure. Although, no gases exactly exhibits ideal behavior, for a large number of gases this approximation is close enough.

If assumptions 1 to 3 hold, then the equations governing the dynamics of pressure and temperature within all the six control volumes (as listed in Table 1) can be depicted on the basis of equations (1)-(2). With turboshaft dynamics accounted for via the speed of the turbocharger, ω_{tc}, following comprehensive 13^{th} order engine model, Σ_1, is obtained [1], [4], [5]:

$$\Sigma_1 = \begin{cases} \dot{P}_{af}(t) = \left(\frac{\gamma R}{V_{af}}\right)\left[\dot{m}_{af_{in}}(t)T_{af_{in}}(t) - \dot{m}_{af_{out}}(t)T_{af}(t)\right] \\ \dot{T}_{af}(t) = \left(\frac{T_{af}(t)}{P_{af}(t)}\right)\left(\frac{\gamma R}{V_{af}}\right)\left[\dot{m}_{af_{in}}(t)T_{af_{in}} - \dot{m}_{af_{out}}(t)T_{af}(t) - \frac{T_{af}(t)}{\gamma}(\dot{m}_{af_{in}} - \dot{m}_{af_{out}})\right] \\ \dot{P}_{c}(t) = \left(\frac{\gamma R}{V_{c}}\right)\left[\dot{m}_{c_{in}}(t)T_{c_{in}}(t) - \dot{m}_{c_{out}}(t)T_{c}(t)\right] \\ \dot{T}_{c}(t) = \left(\frac{T_{c}(t)}{P_{c}(t)}\right)\left(\frac{\gamma R}{V_{c}}\right)\left[\dot{m}_{c_{in}}(t)T_{c_{in}}(t) - \dot{m}_{c_{out}}(t)T_{c}(t) - \frac{T_{c}(t)}{\gamma}(\dot{m}_{c_{in}}(t) - \dot{m}_{c_{out}}(t))\right] \\ \dot{P}_{ic}(t) = \left(\frac{\gamma R}{V_{ic}}\right)\left[\dot{m}_{ic_{in}}(t)T_{ic_{in}}(t) - \dot{m}_{ic_{out}}(t)T_{ic}(t)\right] \\ \dot{T}_{ic}(t) = \left(\frac{T_{ic}(t)}{P_{ic}(t)}\right)\left(\frac{\gamma R}{V_{ic}}\right)\left[\dot{m}_{ic_{in}}(t)T_{ic_{in}}(t) - \dot{m}_{ic_{out}}(t)T_{ic}(t) - \frac{T_{ic}(t)}{\gamma}(\dot{m}_{ic_{in}}(t) - \dot{m}_{ic_{out}}(t))\right] \\ \dot{P}_{im}(t) = \left(\frac{\gamma R}{V_{im}}\right)\left[\dot{m}_{im_{in}}(t)T_{im_{in}}(t) - \dot{m}_{im_{out}}(t)T_{im}(t)\right] \\ \dot{T}_{im}(t) = \left(\frac{T_{im}(t)}{P_{im}(t)}\right)\left(\frac{\gamma R}{V_{im}}\right)\left[\dot{m}_{im_{in}}(t)T_{im_{in}} - \dot{m}_{im_{out}}(t)T_{im}(t) - \frac{T_{im}(t)}{\gamma}(\dot{m}_{im_{in}}(t) - \dot{m}_{im_{out}}(t))\right] \\ \dot{P}_{em}(t) = \left(\frac{\gamma R}{V_{em}}\right)\left[\dot{m}_{em_{in}}(t)T_{em_{in}}(t) - \dot{m}_{em_{out}}(t)T_{em}(t)\right] \\ \dot{T}_{em}(t) = \left(\frac{T_{em}(t)}{P_{em}(t)}\right)\left(\frac{\gamma R}{V_{em}}\right)\left[\dot{m}_{em_{in}}(t)T_{em_{in}}(t) - \dot{m}_{em_{out}}(t)T_{em}(t) - \frac{T_{em}(t)}{\gamma}(\dot{m}_{em_{in}}(t) - \dot{m}_{em_{out}}(t))\right] \\ \dot{P}_{t}(t) = \left(\frac{\gamma R}{V_{t}}\right)\left[\dot{m}_{t_{in}}(t)T_{t_{in}}(t) - \dot{m}_{t_{out}}(t)T_{t}(t)\right] \\ \dot{T}_{t}(t) = \left(\frac{T_{t}(t)}{P_{t}(t)}\right)\left(\frac{\gamma R}{V_{t}}\right)\left[\dot{m}_{t_{in}}(t)T_{t_{in}}(t) - \dot{m}_{t_{out}}(t)T_{t}(t) - \frac{T_{t}(t)}{\gamma}(\dot{m}_{t_{in}}(t) - \dot{m}_{t_{out}}(t))\right] \\ \dot{w}_{tc}(t) = \left(\frac{1}{I_{tc}}\right)(T_{q_t}(t) - T_{q_c}(t) - w_{tc}(t)c_{fr}) \end{cases}$$

where, $T_{q_t}(t)$ represents the driving torque due to the turbine and $T_{q_c}(t)$ denotes the loading torque from the compressor. c_{fr} symbolizes the friction coefficient of the turboshaft. The expressions of mass-flows and inlet temperatures in terms of engine states $P_{cv}(t)$, $T_{cv}(t)$ and $w_{tc}(t)$ are presented in Table 3. Complete details and validation on this can be found in [2] and [4].

Remark 4: This 13^{th} order engine model, Σ_1, does not include some important phenomena like engine oil temperature, engine warm up dependence and wall wetting, that are quite significant for describing the complete engine operation. However, our main aim in this paper is to demonstrate a systematic and rigorous procedure for model reduction. Once a reduced order model has been obtained any additional features can be easily incorporated to account for such phenomena.

3 Model Reduction

In this section we investigate the simplification of the engine model Σ_1 via order reduction. Comprehensive model Σ_1 is deemed to be very effective in examining the behavior of various engine components and carrying out simulation studies. Nevertheless, it is too complex for usage in tasks involving optimization and control using model based techniques. Thus, in order to design improved controllers with the objective of achieving best possible engine performance, model simplification via order reduction is necessary.

The order reduction is accomplished in two stages and is based on the use of perturbation theory [12]. In the development of first lower order model, the dynamic characteristics of pressure and temperature of mass in the control volumes are considered.

Table 3: Control volume mass flows and inlet temperatures

Control Volume	**Mass flow in ($\dot{m}_{cv_{in}}$), mass flow out ($\dot{m}_{cv_{out}}$) and Inlet temperature $\dot{T}_{cv_{in}}$**
Air Filter	$\dot{m}_{af_{in}} = \frac{P_{amb}^2 - P_{af}P_{amb}}{CRT_{af}}$; $\dot{m}_{af_{out}} = \dot{m}_{c_{in}}$; $T_{af_{in}} = T_{amb}$
Compressor	$\dot{m}_{c_{in}} = \left(\frac{P_{af}}{RT_{af}}\frac{\pi}{4}\omega_{tc}\frac{D_c^3}{2}\right)\sqrt{\left(\frac{1-min\left(K_1\left(C_pT_{af}\frac{\left(\frac{P_c}{P_{af}}\right)^{\frac{\gamma-1}{\gamma}}}{\frac{1}{2}\left(\omega_{tc}\frac{D_c}{2}\right)^2}\right)^2,1\right)}{K_2}\right)}$; $\dot{m}_{c_{out}} = \dot{m}_{ic_{in}}$; $T_{c_{in}} = T_{af}\left(1+\frac{\left(\frac{P_c}{P_{af}}\right)-1}{\eta_c}\right)$
Intercooler	$\dot{m}_{ic_{in}} = \frac{P_c^2 - P_{ic}P_c}{CRT_{ic}}$; $\dot{m}_{ic_{out}} = \dot{m}_{im_{in}}$; $T_{ic_{in}} = T_c - \eta_{ic}\left(T_c - T_{amb}\right)$
Intake Manifold	$\Psi\left(\frac{P_{im}}{P_{ic}}\right) = \begin{cases} \frac{\sqrt{\gamma}\left(\frac{2}{\gamma+1}\right)^{\frac{\gamma+1}{2(\gamma-1)}}}{\sqrt{\frac{2\gamma}{\gamma-1}\left(\left(\frac{P_{im}}{P_{ic}}\right)^{\frac{2}{\gamma}} - \left(\frac{P_{im}}{P_{ic}}\right)^{\frac{\gamma+1}{\gamma}}\right)}}, & \frac{P_{im}}{P_{ic}} \leq 0.5283 \\ 1 \geq \frac{P_{im}}{P_{ic}} > 0.5283 \end{cases}$; $\dot{m}_{im_{in}} = \frac{P_{ic}}{\sqrt{RT_{ic}}}A_e(\alpha)\Psi\left(\frac{P_{im}}{P_{ic}}\right)$; $\dot{m}_{im_{out}} = \frac{P_{im}V_d n_{cyl}\eta_{vol}N_{rps}}{4\pi RT_{im}}$; $T_{im_{in}} = T_{ic}$;
Exhaust manifold	$\dot{m}_{em_{in}} = \dot{m}_{im_{out}}\left(1+\frac{1}{\lambda\left(\frac{A}{F}\right)_s}\right)$; $\dot{m}_{em_{out}} = \dot{m}_{t_{in}}$;
Turbine	$\Psi_t\left(\frac{P_t}{P_{em}}\right) = \begin{cases} \frac{\sqrt{\gamma_{eg}}\left(\frac{2}{\gamma_{eg}+1}\right)^{\frac{\gamma_{eg}1}{2(\gamma_{eg}-1)}}}{\sqrt{\frac{2\gamma_{eg}}{\gamma_{eg}-1}\left(\left(\frac{P_t}{P_{em}}\right)^{\frac{2}{\gamma_{eg}}} - \left(\frac{P_t}{P_{em}}\right)^{\frac{\gamma_{eg}+1}{\gamma_{eg}}}\right)}}, & \frac{P_t}{P_{em}} \leq 0.5283 \\ 1 \geq \frac{P_t}{P_{em}} > 0.5283 \end{cases}$; $\dot{m}_{t_{in}} = \dot{m}_t + \dot{m}_{wg}$; $\dot{m}_t = \frac{P_{em}}{\sqrt{T_{em}}}k_{t_1}\sqrt{1-\left(\frac{P_t}{P_{em}}\right)^{k_{t_2}}}$; $\dot{m}_{wg} = \frac{P_{em}}{\sqrt{RT_{em}}}\Psi_t\left(\frac{P_t}{P_{em}}\right)C_dA_{wg_{max}}u_{wg}$; $\dot{m}_{t_{out}} = \frac{P_t^2 - P_tP_{amb}}{CRT_t}$

Whereas stage 3 model reduction is based on the physical magnitudes. Subsections 3.1 and 3.2 below deal with the stage 2 and stage 3 model reductions, respectively.

3.1 Stage 2 Engine Model: Model reduction I

This model simplification is based on the observation that in all the engine control volumes the magnitude of the derivative of pressure is significantly larger in comparison to the magnitude of derivative of temperature. This difference in magnitudes can be attributed to the $\left(\frac{T_{cv}(t)}{P_{cv}(t)}\right)$ term in (2). Typically, the ratio $\left(\frac{T_{cv}(t)}{P_{cv}(t)}\right)$ in the context of engine control volumes is a very small positive quantity. Since variations in the temperatures are negligibly small in comparison to the pressures, temperatures can be thought to belong to a compact set which contains the equilibrium point ($T_{cv_{in}}(t)$ in this case). In order to investigate this time scale separation let us rewrite equations (1)-(2), which govern the dynamics of temperature and pressure in each control volume, in the following form:

$$\dot{P}_{cv}(t) = f(t, P_{cv}(t), T_{cv}(t)) \tag{3}$$

$$\dot{T}_{cv}(t) = \varepsilon_{T_{cv}}(t) g(t, P_{cv}(t), T_{cv}(t)) \tag{4}$$

where,

$\varepsilon_{T_{cv}}(t) = \left(\frac{T_{cv}(t)}{P_{cv}(t)}\right)$, $f(t, P_{cv}(t), T_{cv}(t)) = \left(\frac{\gamma R}{V}\right)\left[\dot{m}_{in}(t) T_{cv_{in}}(t) - \dot{m}_{out}(t) T_{cv}(t)\right]$ and

$g(t, P_{cv}(t), T_{cv}(t)) = \left(\frac{\gamma R}{V}\right)\left[\dot{m}_{in}(t) T_{cv_{in}}(t) - \dot{m}_{out}(t) T_{cv}(t) - \frac{T_{cv}(t)}{\gamma}(\dot{m}_{in}(t) - \dot{m}_{out}(t))\right]$.

Since the values of temperatures and pressures in engine control volumes are strictly positive finite quantities, it is easy to say that there exists $0 < \varepsilon^* < \infty$ such that

$\forall\ cv \in [af, c, ic, im, em, t]$

$$\varepsilon_{T_{cv}}(t) \leq \varepsilon^* \qquad \forall t \geq 0 \tag{5}$$

Furthermore, if $\varepsilon_{T_{cv}}(t)_{max}$ and $\varepsilon_{T_{cv}}(t)_{min}$ denote the maximum and minimum values of $\varepsilon_{T_{cv}}(t)$ (for each control volume), respectively, then its average value, $\varepsilon_{av_{cv}}$, becomes

$$\varepsilon_{av_{cv}} = \frac{\varepsilon_{T_{cv}}(t)_{max} + \varepsilon_{T_{cv}}(t)_{min}}{2} \tag{6}$$

From (5) and (6), we deduce that $\exists\ \Delta\varepsilon_{T_{cv}}(t)$, which signifies the variation of $\varepsilon_{T_{cv}}(t)$ from its average value, such that

$$\varepsilon_{T_{cv}}(t) = \varepsilon_{av_{cv}} + \Delta\varepsilon_{T_{cv}}(t) \qquad \forall t \geq 0 \tag{7}$$

By substituting (7) in (4) we obtain

$$\dot{T}_{cv}(t) \;\; = \;\; \varepsilon_{av_{cv}} g(t, P_{cv}(t), T_{cv}(t)) + \Delta\varepsilon_{T_{cv}}(t) g(t, P_{cv}(t), T_{cv}(t)) \tag{8}$$

Assumption 4 The magnitude of $\Delta\varepsilon_{T_{cv}}(t)$ in all engine control volume is sufficiently small in comparison to $\varepsilon_{av_{cv}}$.

Assumption 5 The magnitude of $\varepsilon_{av_{cv}}$ is sufficiently small.

Remark 5: Satisfaction of Assumption 4 with a sufficiently small $\Delta\varepsilon_{T_{cv}}(t)$ allows for the effective use of *regular perturbation theory* to obtain a simplified engine model (which yields an approximate response) [12]. This concept has been further elucidated by means of Theorem 1 later in this section. One way to analytically evaluate the effect of smallness of $\Delta\varepsilon_{T_{cv}}(t)$ on closeness of the approximate solution to the actual solution is to examine the upper bound on the nominal $\Delta\varepsilon_{T_{cv}}(t)$ fluctuations as shown below.

By denoting

$$\frac{\varepsilon_{T_{cv}}(t)_{min}}{\varepsilon_{T_{cv}}(t)_{max}} = \lambda_{cv} \tag{9}$$

it is straightforward to note that

$$\frac{\Delta\varepsilon_{T_{cv}}(t)}{\varepsilon_{av_{cv}}} \leq \frac{(1-\lambda_{cv})}{(1+\lambda_{cv})} \equiv K_{cv} \tag{10}$$

Since, $\lambda \in [0,1]$ we have $K_{cv} \in [0,1]$. Further, in the case at hand $\varepsilon_{T_{cv}}(t)_{min} > 0$ is always true, therefore, it can be concluded that $K_{cv} < 1$ also holds for all times. In order for the simplified model to be a good approximation of the original control volume dynamic description, (3)-(4), the bounding factor K_{cv} should be as small as possible. Smaller the value of K_{cv}, closer will be the dynamic and steady state responses of the approximating system to the original system. Moreover, when $K_{cv} = 0$ the approximating system is the exact copy of the original system. Some sample plots, where K_{cv} is plotted for various control volumes under widely changing operating conditions, are demonstrated in figure 2. The simulation results depict the worst case scenario as the throttle position is varied from almost closed to wide open. It is clear from the simulation results that $\left(\frac{\Delta\varepsilon_{T_{cv}}}{\varepsilon_{av_{cv}}}\right)$ is upperbounded by K_{cv} for all control volumes and K_{cv} itself is much smaller than one. So, it can be deduced that magnitude of $\Delta\varepsilon_{T_{cv}}$ is much smaller that $\varepsilon_{av_{cv}}$ under all operating condition.

Remark 6: Figure 2 shows the plot $\varepsilon_{T_{cv}}(t)$ and $\varepsilon_{av_{cv}}$ for all six control volumes. It is easy to see that the the magnitude of $\varepsilon_{av_{cv}}$ in all the cases is of the order 10^{-3} and therefore in the context of engine can be seen as sufficiently small. This permits the implementation of *singular perturbation theory* for model order reduction (demonstrated later in this section) [12].

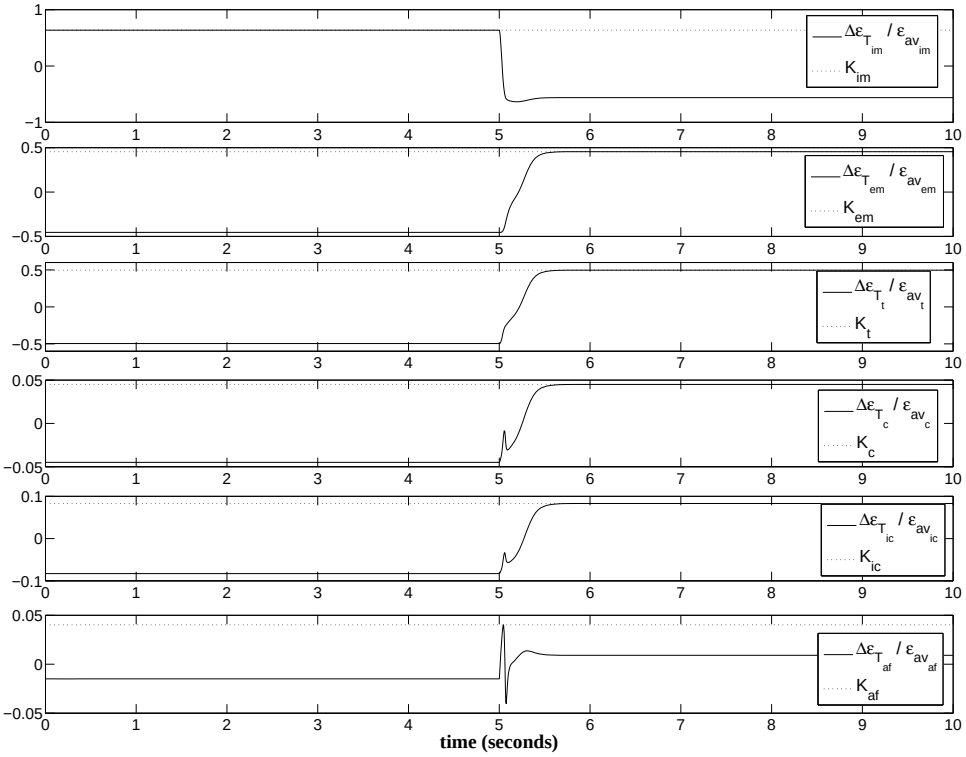

Figure 2: $\frac{\Delta\varepsilon_{T_{cv}}}{\varepsilon_{av_{cv}}}$ and K_{cv} responses for all engine control volumes

In light of Remarks 5 and 6 above, it is reasonable to assume that the assumptions 4 and 5 are satisfied.

Due to the smallness of $\Delta\varepsilon_{T_{cv}}(t)$, solving equation (8) can be seen as a *regular perturbation* problem. The smallness of $\Delta\varepsilon_{T_{cv}}(t)$ will now be exploited to establish an approximate solution to (8).

By setting $\Delta\varepsilon_{T_{cv}}(t) = 0$, the following nominal or unperturbed system is obtained:

$$\dot{\bar{T}}_{cv}(t) \quad = \quad \varepsilon_{av_{cv}} g(t, P_{cv}(t), \bar{T}_{cv}(t)) \qquad \bar{T}_{cv}(t_0) = \bar{T}_{cv_0} \tag{11}$$

where, $\bar{T}_{cv}(t)$ represents the temperature.

The closeness of solutions of dynamic equations (8) and (11) is ensured by following Theorem 3.4 of [12]. With respect to the engine setup, this result can be expressed in the form of Theorem 1 below.

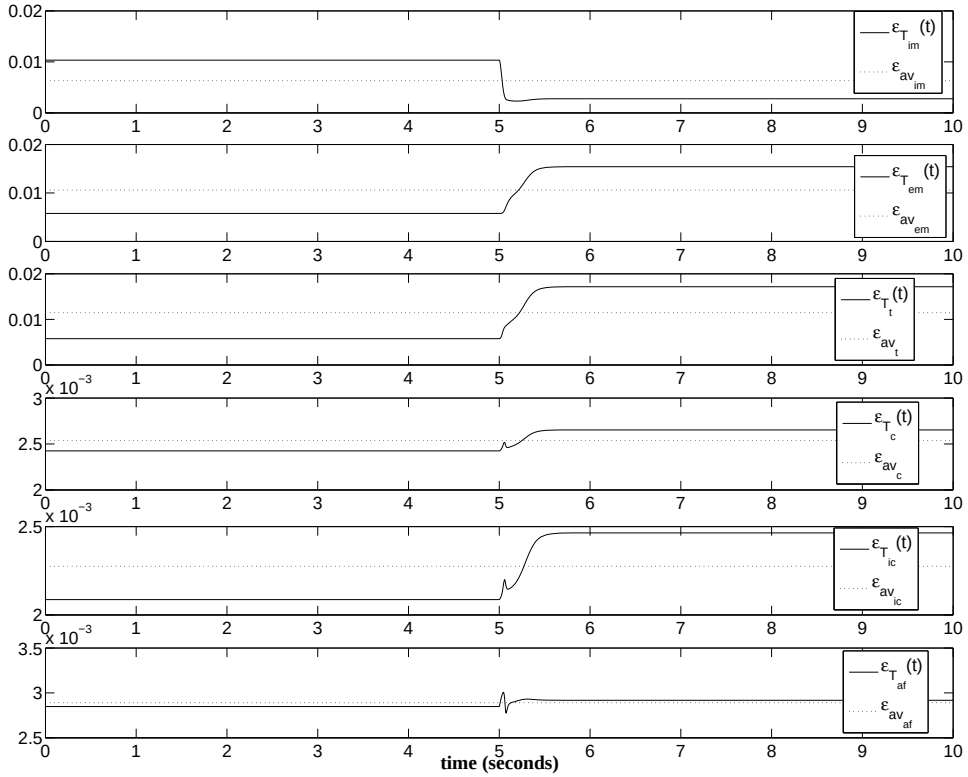

Figure 3: $\varepsilon_{T_{cv}}(t)$ and $\varepsilon_{av_{cv}}$ responses for all engine control volumes

Theorem 1 *Let $\varepsilon_{av_{cv}} g(t, P_{cv}(t), \bar{T}_{cv}(t))$ be piecewise continuous in t and Lipschitz in $\bar{T}_{cv}(t)$ on $[t_0, t_1] \times W$ with a Lipschitz constant L, where $W \subset R^6$ is an open connected set. Let $\bar{T}_{cv}(t)$ and $T_{cv}(t)$ be solution of*

$$\dot{\bar{T}}_{cv}(t) \;=\; \varepsilon_{av_{cv}} g(t, P_{cv}(t), \bar{T}_{cv}(t)), \qquad \bar{T}_{cv}(t_0) = \bar{T}_{cv_0}$$

and

$$\dot{T}_{cv}(t) \;=\; \varepsilon_{av_{cv}} g(t, P_{cv}(t), T_{cv}(t)) + \Delta\varepsilon_{T_{cv}}(t) g(t, P_{cv}(t), T_{cv}(t)), \quad T_{cv}(t_0) = T_{cv_0}$$

such that $\bar{T}_{cv}(t), T_{cv}(t) \in W$ for all $t \in [t_0, t_1]$. Suppose that

$$\Delta\varepsilon_{T_{cv}}(t) g(t, P_{cv}(t), T_{cv}(t)) \leq \mu \|\varepsilon^* - min(\varepsilon_{av_{cv}})\|, \quad \forall\ (t, T_{cv}(t)) \in [t_0, t_1] \times W$$

for some $\mu > 0$. Then,

$$\|\bar{T}_{cv}(t) - T_{cv}(t)\| \leq \|\bar{T}_{cv_0} - T_{cv_0}\| exp[L(t - t_0)] + \frac{\|\varepsilon^* - min(\varepsilon_{av_{cv}})\|\mu}{L} \{exp[L(t - t_0)] - 1\}$$

Hence, the overall system control volume dynamics, (3)-(4), can be approximated by the following set of equations

$$\dot{P}_{cv}(t) = f(t, P_{cv}(t), \bar{T}_{cv}(t)) \tag{12}$$

$$\dot{\bar{T}}_{cv}(t) = \varepsilon_{av_{cv}} g(t, P_{cv}(t), \bar{T}_{cv}(t)) \tag{13}$$

Further, by simple change of time variable equations (12)-(13) can be expressed in standard singularly perturbed form as

$$\varepsilon_{av_{cv}} \dot{P}_{cv}(\tau) = f(\tau, P_{cv}(\tau), \bar{T}_{cv}(\tau)) \tag{14}$$

$$\dot{\bar{T}}_{cv}(\tau) = g(\tau, P_{cv}(\tau), \bar{T}_{cv}(\tau)) \tag{15}$$

The system description (14)-(15) is in standard *singularly perturbed form* and demonstrates the time scale separation between the dynamics of pressure and temperature [12]. Specifically, the dynamics of pressure are much faster than those of temperature. The usual practice in singular perturbation theory is to approximate the fast dynamic with its quasi steady state value and reduce the order of the system by considering only slow dynamic. In this case, we pursue the alternative direction by focusing on the fast dynamic (pressure) and approximating the slow dynamic (temperature) by its quasi steady state value. This course of action is motivated by the following:

The transient fluctuations in temperatures are much smaller than those in pressures. This makes approximation of temperatures a more viable choice. From (2) it is easy to see that the steady state value (equilibrium point) of control volume temperatures is equal to the temperature of the gases at the inlet (as at equilibrium $\dot{m}_{cv_{in}} = \dot{m}_{cv_{out}}$). Inlet temperatures, in turn, are typically functions

of pressures. As a result, excluding temperatures ($T_{cv}(t)$) from the state vector and replacing them by their quasi-steady state values ($T_{cv_{in}}(t)$ in this case) allows the complete engine to be described by fewer state variables.

Therefore, we retain the $P_{cv}(\tau)$ as the state to obtain the reduced order system as

$$\dot{P}_{cv}(\tau) = f(\tau, P_{cv}(\tau), T_{cv_{in}}(\tau, P_{cv}(\tau))) \tag{16}$$

$$0 = g(\tau, P_{cv}(\tau), \bar{T}_{cv}(\tau)) \tag{17}$$

Let the solution of (16) be represented as $\bar{P}_{cv}(\tau)$. Since, the temperature variable $\bar{T}_{cv}(\tau)$ has been eliminated and replaced by its quasi-steady value $T_{cv_{in}}(\tau, \bar{P}_{cv}(\tau))$, the only information we can obtain about $\bar{T}_{cv}$ by solving (16) is determined as

$$\tilde{T}_{cv}(\tau) = T_{cv_{in}}(\tau, \bar{P}_{cv}(\tau)) \tag{18}$$

where, $\tilde{T}_{cv}(\tau)$ represents the quasi-steady state behavior of $\bar{T}_{cv}(\tau)$ when $P_{cv}(\tau) = \bar{P}_{cv}(\tau)$. The important point to note here is that $T_{cv_{in}}(\tau, \bar{P}_{cv}(\tau))$ is not free to start from a prescribed initial condition and hence does not represent a uniform approximation of $\bar{T}_{cv}(\tau)$. The best we can expect is to check the stability properties of $\left[\bar{T}_{cv}(\tau) - \bar{T}_{cv_{in}}(\tau, \bar{P}_{cv}(\tau))\right]$ and in that ensuring that the $\tilde{T}_{cv}(\tau)$ (or $\bar{P}_{cv}(\tau)$) remains sufficiently close to $\bar{T}_{cv}(\tau)$ (or $\bar{P}_{cv}(\tau)$) during the desired interval of time.

By denoting $y(\tau) = \bar{T}_{cv}(\tau) - T_{cv_{in}}(\tau, \bar{P}_{cv}(\tau))$, the error dynamics are yielded as

$$\dot{y}(\tau) = \dot{\bar{T}}(\tau) - \dot{T}_{cv_{in}}(\tau, \bar{P}_{cv}(\tau)) \tag{19}$$

Then, the closeness of solution of (14)-(15) to (16) can be established by Theorem 11.1 of [12] (commonly known as *Tikhnov's theorem*) which, in the case at hand, can be stated as follow:

Theorem 2 *Consider the singular perturbation problem of (14)-(15) and let* $\bar{T}_{cv}(\tau) = T_{cv_{in}}(\tau, P_{cv}(\tau))$ *be an isolated root of (17). Assume that the following conditions are satisfied for all*

$$\left[\tau, P_{cv}(\tau), \bar{T}_{cv} - T_{cv_{in}}(\tau, P_{cv}(\tau)), \varepsilon_{av_{cv}}\right] \in [0, \tau_1] \times D_{P_{cv}} \times D_y \times [0, \varepsilon_0]$$

for some domains $D_{P_{cv}} \subset \mathcal{R}^n$ *and* $D_y \subset \mathcal{R}^m$ *in which* $D_{P_{cv}}$ *is convex and* D_y *contains the origin:*

- *The functions* f, g*, their first partial derivatives with respect to* $\left(P_{cv}, \bar{T}_{cv}, \varepsilon_{av_{cv}}\right)$*, and the first partial derivative of* g *with respect to* τ *are continuous, the function* $T_{cv_{in}}(\tau, P_{cv}(\tau))$ *and the jacobian* $[\partial g(\tau, P_{cv}, \bar{T}_{cv})/\partial \bar{T}_{cv}]$ *have continuous first partial derivatives with respect to their arguments.*

- *The reduced order system (16) has a unique solution* $\bar{P}_{cv}(\tau) \in S$*, for* $\tau \in [\tau_0, \tau_1]$*, where* S *is a compact subset of* $D_{P_{cv}}$*.*

- *The origin is an exponentially stable equilibrium point of the boundary-layer model (17), uniformly in* (τ, P_{cv})*; let* $M \subset D_y$ *be the region of attraction of (17) and* Ω_y *be a compact subset of* M*.*

Then, there exits a positive constant $\varepsilon^*_{av_{cv}}$ *such that for all* $\bar{T}_{cv}(\tau_0) - T_{cv_{in}}(\tau_0, P_{cv}(\tau_0)) \in \Omega_y$ *and* $0 < \varepsilon_{av_{cv}} < \varepsilon^*_{av_{cv}}$*, the singular perturbation problem of (14)-(15) has a unique solution of* $P_{cv}(\tau)$*,* $\bar{T}_{cv}(\tau)$ *on* $[t_0, t_1]$*, and*

$$P_{cv}(\tau) - \bar{P}_{cv}(\tau) = O(\varepsilon_{av_{cv}}) \tag{20}$$

$$T_{cv}(\tau) - T_{cv_{in}}(\tau, \bar{P}_{cv}(\tau)) - \hat{y}(\tau) = O(\varepsilon_{av_{cv}}) \tag{21}$$

holds uniformly for $\tau \in [\tau_0, \tau_1]$*, where* $\hat{y}(\tau)$ *is the solution of (17). Moreover, given any*

$\tau_b > \tau_0$, *there exists* $\varepsilon^{**}_{av_{av}} \leq \varepsilon_{av_{cv}}$ *such that*

$$\bar{T}_{cv}(\tau) - T_{cv_{in}}(\tau, \bar{P}_{cv}(\tau)) = O(\varepsilon_{av_{cv}}) \tag{22}$$

holds uniformly for $\tau \in [\tau_b, \tau_1]$ *whenever* $\varepsilon_{av_{cv}} < \varepsilon^{**}_{av_{cv}}$.

Thus following (16), the stage 2 model (Σ_2) (in original time variable t) obtained after the first reduction can be approximated as the following 7^{th} order system:

$$\Sigma_2 = \begin{cases} \dot{P}_{af}(t) = \left(\frac{\gamma R T_{af_{in}}(t)}{V_{af}}\right)[\dot{m}_{af_{in}}(t) - \dot{m}_{af_{out}}(t)] \\ \dot{P}_{c}(t) = \left(\frac{\gamma R T_{c_{in}}}{V_{c}}\right)[\dot{m}_{c_{in}}(t) - \dot{m}_{c_{out}}(t)] \\ \dot{P}_{ic}(t) = \left(\frac{\gamma R T_{ic_{in}}(t)}{V_{ic}}\right)[\dot{m}_{ic_{in}}(t) - \dot{m}_{ic_{out}}(t)] \\ \dot{P}_{im}(t) = \left(\frac{\gamma R T_{im_{in}}(t)}{V_{im}}\right)[\dot{m}_{im_{in}}(t) - \dot{m}_{out}(t)] \\ \dot{P}_{em}(t) = \left(\frac{\gamma R T_{em_{in}}(t)}{V_{em}}\right)[\dot{m}_{em_{in}}(t) - \dot{m}_{em_{out}}(t)] \\ \dot{P}_{t}(t) = \left(\frac{\gamma R T_{t_{in}}(t)}{V_{t}}\right)[\dot{m}_{t_{in}}(t) - \dot{m}_{t_{out}}(t)] \\ \dot{w}_{tc}(t) = \left(\frac{1}{I_{tc}}\right)(T_{q_t}(t) - T_{q_c}(t) - w_{tc}(t)c_{fr}) \end{cases}$$

Remark 7: It is interesting to note that $\varepsilon_{T_{cv}}(t)$ is always a very small number and is bounded within the interval of the order 10^{-3} (as shown in Figure 3). This allows for the use of time varying singular perturbation parameters.

3.1.1 Comparison of Σ_1 and Σ_2

In this subsection, we examine the errors in the pressures and temperatures introduced by reducing the order of engine model Σ_1 and to engine model Σ_2. Figures 4 and 5 show the deviations in the responses of pressures and temperatures when the temperature dynamics are excluded and replaced by their quasi-steady state values. In the simulation, we assume that at time $t = 5s$ a step change in throttle takes place whereby

the throttle status changes from almost closed to wide open. This is followed by instantaneous opening of wastegate at time $t = 10s$. It is clear from the error responses that the behavior of pressures and temperatures generated by Σ_1 and Σ_2 are identical in steady state. On the other hand, as expected the values are different during the transient phases but the errors are quite small.

Due to the non-zero errors during the transient phases, Σ_2 cannot be seen as a *perfect* representation of Σ_1. However, since Σ_2 introduces only a negligible error relative to the original 13^{th} order validated model, Σ_1, it can be treated as a good representation for all practical purposes including controller design.

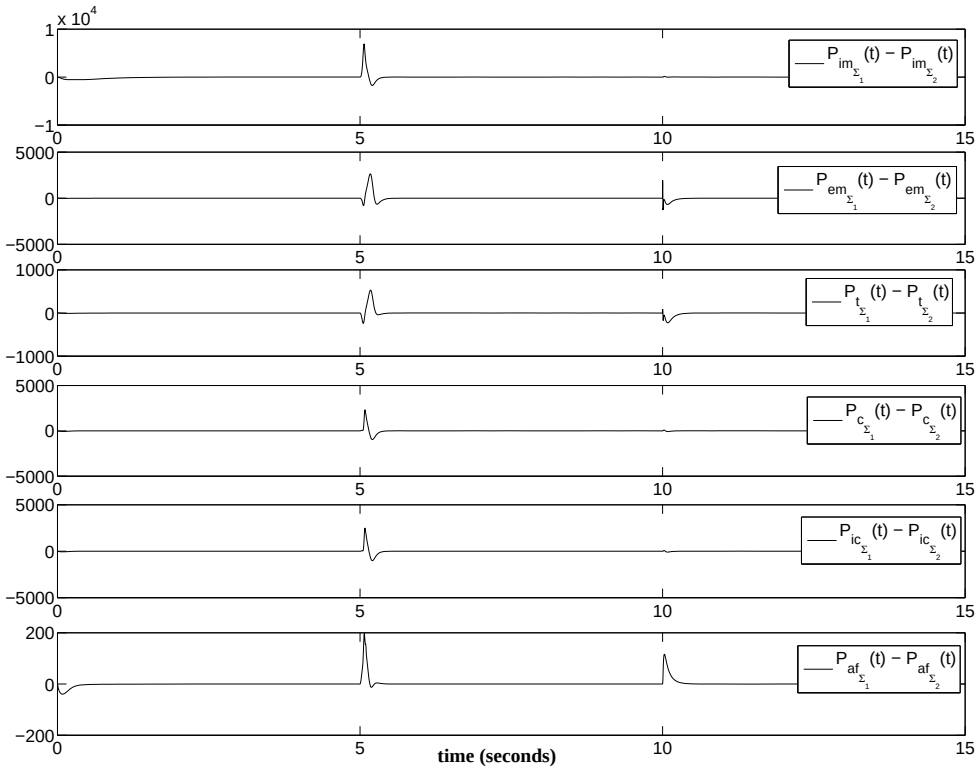

Figure 4: Discrepancies in pressure responses due to Σ_1 and Σ_2

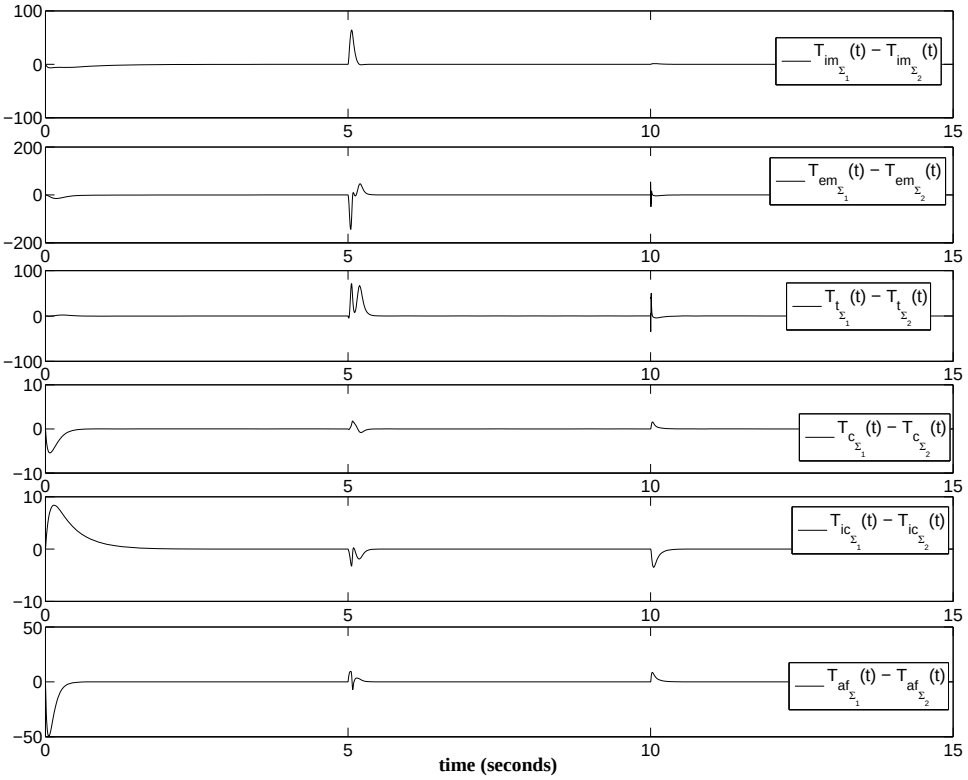

Figure 5: Discrepancies in temperature responses due to Σ_1 and Σ_2

3.2 Stage 3 Engine Model: Model Reduction II

In this section, we explore the possibility of further model reduction of engine model Σ_2 derived in the previous section. While reductions leading to Σ_2 are based on the dynamic characteristics of engine control volumes, now we consider their physical properties, specifically, the relative control volumes. The motivation for this follows from the fact that the magnitude of the pressure dynamics is inversely proportional to volume V_{cv}. Thus, smaller V_{cv} will lead to faster transients and hence there exists a time scale separation within the dynamics of control volume pressures. In order to conceptualize this argument, let us rewrite the equation (16) as follows:

$$\dot{P}_{cv}(t) \;=\; \frac{1}{\varepsilon_{P_{cv}}}\left(\frac{\gamma R T_{cv_{in}}}{V_{max}}\right)\left[\dot{m}_{cv_{in}}(t) - \dot{m}_{cv_{out}}(t)\right] \tag{23}$$

where, $\varepsilon_{P_{cv}} = \left(\frac{V_{cv}}{V_{max}}\right)$ and $V_{max} = max(V_{im}, V_{em}, V_t, V_c, V_{ic})$.

Assumption 6 There is a sufficiently large difference in the sizes of various engine control volume reservoirs.

Assumption 7 The volumes of intercooler control volume, intake manifold and exhaust manifold are sufficiently larger than those of air filter, compressor and turbine contol volumes and the turbine control volume is the smallest.

Remark 8: Assumption 6 holds without loss of generality as the sizes of various engine control volumes are usually sufficiently different in production engines. On the other hand, assumption 7 is justified as in the context of turbocharged engine, sizes of intake manifold, exhaust manifold and intercooler control volumes are typically much larger than those of turbine, compressor and air filter with turbine control volume being the smallest. In the situations where this is not strictly true, an alternative assumption can be made and the same procedure for model reduction can be adopted.

As a result, the reduced order model Σ_2 can be rewritten depicting the time scale separation due to the different volume magnitudes in the following singularly perturbed form:

$$\dot{P}_1(t) = f_{ic,im,em}\left(P_1(t), P_2(t), w_{tc}(t)\right) \tag{24}$$

$$\varepsilon_t \dot{P}_2(t) = f_{af,c,t}\left(P_1(t), P_2(t), w_{tc}(t)\right) \tag{25}$$

where,

$$P_1(t) = \begin{bmatrix} P_{ic}(t) & P_{im}(t) & P_{em}(t) \end{bmatrix}^T, \; P_2(t) = \begin{bmatrix} P_{af}(t) & P_c(t) & P_t(t) \end{bmatrix}^T,$$

$$f_{ic,im,em}\left(P_1(t), P_2(t), w_{tc}(t)\right) = \begin{bmatrix} \frac{\gamma R T_{ic_{in}}(t)}{V_{max}}\left(\dot{m}_{ic_{in}}(t) - \dot{m}_{ic_{out}}(t)\right) \\ \frac{\gamma R T_{im_{in}}(t)}{V_{max}}\left(\dot{m}_{im_{in}}(t) - \dot{m}_{im_{out}}(t)\right) \\ \frac{\gamma R T_{em_{in}}}{V_{max}}\left(\dot{m}_{em_{in}}(t) - \dot{m}_{em_{out}}(t)\right) \end{bmatrix} \text{ and}$$

$$f_{af,c,t}\left(P_1(t), P_2(t), w_{tc}(t)\right) = \begin{bmatrix} \left(\frac{\varepsilon_t}{\varepsilon_{af}}\right)\left(\frac{\gamma R T_{amb}}{V_{max}}\right)\left(\dot{m}_{af_{in}}(t) - \dot{m}_{af_{out}}(t)\right) \\ \left(\frac{\varepsilon_t}{\varepsilon_c}\right)\left(\frac{\gamma R T_{comp_{in}}}{V_{max}}\right)\left(\dot{m}_{comp_{in}}(t) - \dot{m}_{comp_{out}}(t)\right) \\ \left(\frac{\gamma R T_{t_{in}}}{V_{max}}\right)\left(\dot{m}_{t_{in}}(t) - \dot{m}_{t_{out}}(t)\right) \end{bmatrix}.$$

As a consequence of assumption 6 and 7, we have ε_t to be sufficiently small. The smallness of ε_t allows the application of singular perturbation theory and, hence, dynamics of $P_2(t)$ can be approximated by their quasi-steady value. By setting $\varepsilon_t = 0$, from (25) we obtain

$$0 = f_{af,c,t}\left(P_1(t), P_2(t), w_{tc}(t)\right) \tag{26}$$

Solution of (26) for $P_2(t)$ in terms of $P_1(t)$ and $w_{tc}(t)$ yields its quasi-steady state value which can be expressed in the following form:

$$P_{af}(t) = g_{af}\left(t, P_2(t), \omega_{tc}(t)\right) \tag{27}$$

$$P_c(t) = g_c\left(t, P_2(t), \omega_{tc}(t)\right) \tag{28}$$

$$P_t(t) = g_t\left(t, P_2(t), \omega_{tc}(t)\right) \tag{29}$$

where, functions $g_{af}\left(t, P_2(t), \omega_{tc}(t)\right)$, $g_c\left(t, P_2(t), \omega_{tc}(t)\right)$ and $g_t\left(t, P_2(t), \omega_{tc}(t)\right)$ are approximated by expanding $f_{af,c,t}\left(P_1(t), P_2(t), w_{tc}(t)\right)$ in its Taylor series and solving it for $P_2(t)$ by equating it to zero. The existence of a unique solution of (26) is ascertained by the application of *implicit function theorem* [9].

The reduced order stage 3 model thus obtained after the exclusion of fast pressures and replacing them with their quasi-steady state values of the form (27)-(29) is given

by

$$\Sigma_3 = \begin{cases} \dot{P}_{ic}(t) = \left(\frac{\gamma R T_{ic_{in}}(t)}{V_{ic}}\right)\left[\dot{m}_{ic_{in}}(t) - \dot{m}_{ic_{out}}(t)\right] \\ \dot{P}_{im}(t) = \left(\frac{\gamma R T_{im_{in}}(t)}{V_{im}}\right)\left[\dot{m}_{im_{in}}(t) - \dot{m}_{out}(t)\right] \\ \dot{P}_{em}(t) = \left(\frac{\gamma R T_{em_{in}}(t)}{V_{em}}\right)\left[\dot{m}_{em_{in}}(t) - \dot{m}_{em_{out}}(t)\right] \\ \dot{w}_{tc}(t) = \left(\frac{1}{I_{tc}}\right)\left(T_{q_t}(t) - T_{q_c}(t) - w_{tc}(t)c_{fr}\right) \end{cases}$$

Remark 9: It may be noted that whereas Σ_2 is obtained by considering the fast dynamics (control volume pressures) and eliminating the slow dynamics (control volume temperatures), Σ_3 is derived by getting rid of the fast pressures and considering the slow ones. Thus, to obtain reduced order model Σ_3 from Σ_1 we are focusing on the *middle* time scale. Middle time scale is physically most relevant time scale with respect to both slow as well as fast time scales. The control inputs, throttle angle and waste gate control, which play a vital role in the control design are directly associated with the dynamical equations governing the variables in the middle time scale, namely P_{ic}, P_{im} and P_{em}. Furthermore, conceptually control oriented mean value model should capture the average behavior and, hence, considering middle time scale is more feasible from the point of view of controller design.

3.2.1 Comparison of Σ_1 and Σ_3

As in stage 2 model reduction, the key to the accuracy of stage 3 engine model Σ_3 lies in the accuracy with which the fast pressure, $P_{af}(t), P_c(t), P_t(t)$ can be approximated.

In this section we demonstrate the solution of (26) using Taylor series expansion (shown in figures 6, 7 and 8). It is easy to see that the solution of Σ_3 approaches Σ_1 as the order of approximation is increased. It is worth pointing out that the authors had

to stop at 5^{th} order approximation due to the computational and display limitations of MATLAB symbolic toolbox. With an alternative computational tool, it may be possible to achieve even higher level of accuracy.

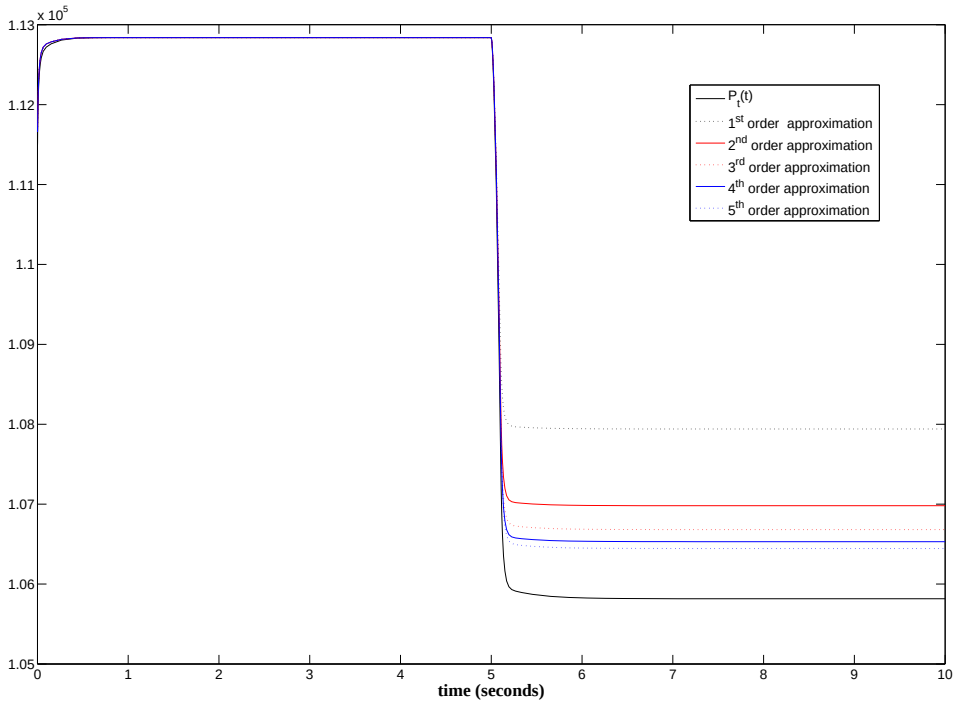

Figure 6: Approximation of turbine pressure

4 Conclusions

In this paper, a novel technique to obtain reduced order engine models is demonstrated. It is constructively shown that if certain set of assumptions are satisfied then it is possible to sequentially eliminate some of the state variable and represent the engine behavior by fewer states to obtain reduced order models. The assumptions, imposed on the physical and dynamic characteristics of the engine, are found to hold quite well. Model reduction is achieved by the application of perturbation theory, first to

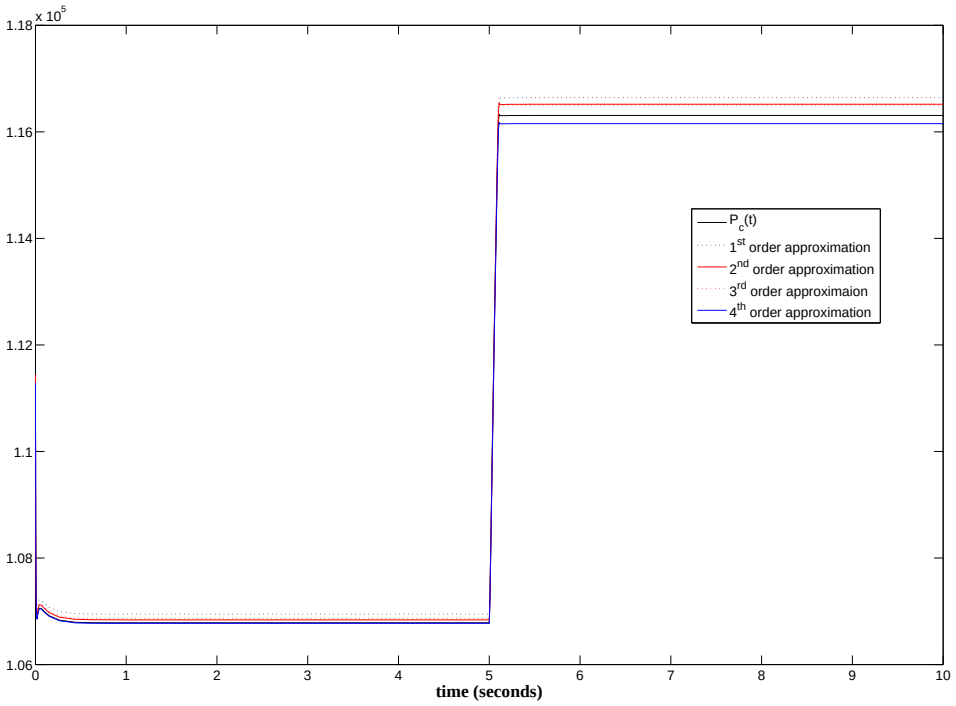

Figure 7: Approximation of compressor pressure

eliminate slow temperatures and then to reject fast pressures. The main advantage of this modeling approach is that it is based on the solid theoretical basis and as a result the reduced order models closely approximate the original model under a wide range of operating conditions. Moreover, the obtained model, because they heavily rely on physical laws rather than empirical findings, can be carried to represent a number of different engines.

While investigating the model reduction a number of interesting modeling scenarios are revealed. In the situations where the ratio of temperature and pressure stays relatively constant with the changing operating conditions, reduction from Σ_1 to Σ_2 is an accurate description of true behavior. Further, if the difference in the relative sizes of various control volumes is large, reduced order model Σ_3 is a closer description of

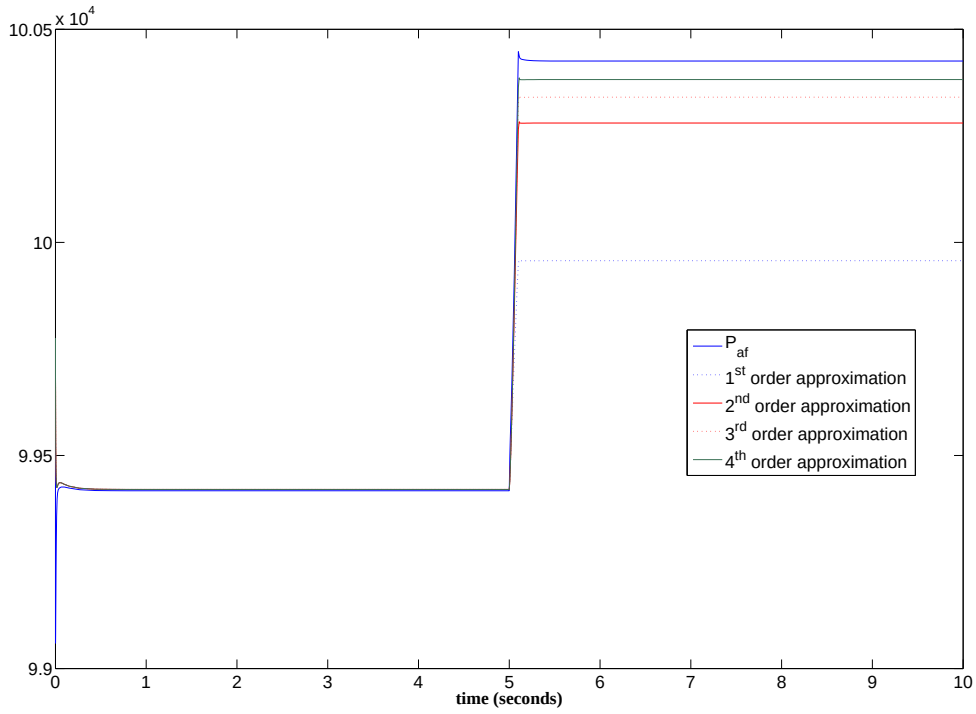

Figure 8: Approximation of air filter pressure

Σ_2. It is also interesting to note that the reduction from Σ_1 to Σ_3 can also be directly directly in the situations where the assumptions leading to Σ_2 cannot be guaranteed but those necessary for Σ_3 hold. In the rare situations where any of these assumptions do not hold then an alternative model reduction approach should be adopted.

5 Acknowledgements

This work was supported by Energy Technology Innovation Strategy (ETIS) and Advanced Centre for Automotive Research and Testing (ACART) at The University of Melbourne, Australia.

References

[1] P. Andersson. *Air charge estimation in turbocharged spark ignition engines*. PhD thesis, Department of Electrical Engineering, Linkoping University, 2005.

[2] P. Andersson and L. Eriksson. Cylinder air charge estimator in turbocharged si-engine. *SAE Technical Paper 2004-01*, 2004.

[3] L. Eriksson, S. Frie, C. Onder, and L. Guzzella. Control and optimization of turbocharged spark ignited engines. In *15th Trinnial World Congress, Barcelona, Spain*, 2002.

[4] Lars Eriksson, Lars Nielson, Jan Brugard, Johan Bergstrom, Fredrick Pettersson, and Per Andersson. Modeling of a turbocharged spark ignition engine. *Annual Reviews in Control*, 26:129–137, 2002.

[5] S. Frei. *Performance and driveability optimization of turbocharged engine systems*. PhD thesis, Technische Wissenschaften, Eidgenssische Technische Hochschule ETH Zrich, 2004.

[6] L. Guzzella and C.H. Onder. *Introduction to Modeling and Control of Internal Combustion Engine*. Springer, 2004.

[7] Elbert Hendricks. Engine modelling for control applications: a critical survey. *Meccanica*, 32(5):387–396, 1997.

[8] J.B. Heywood. *Internal Combustion Engine Fundamentals*. McGraw Hill, 1988.

[9] Alberto Isidori. *Nonlinear control systems*. Berlin ; New York : Springer, 1995.

[10] M. Jankovic and I. Kolmanovsky. Constructive lyapunov control design for turbocharged diesel engines. *IEEE Transactions on Control System Technology*, 8(2):288–299, March 2000.

[11] J.P. Jensen, A.F. Kristensen, S.C. Sorenson, N. Houbak, and E. Hendricks. Mean value modeling of a small turbocharged diesel engine. *SAE 910070*.

[12] Hassan K Khalil. *Nonlinear Systems*. Prentice Hall, 3rd edition, 2002.

[13] D. Khiar, J. Lauber, T.M. Guerra, T. Floquet, Y. Chamaillard, and G. Colin. Nonlinear modeling and control approach for a turbocharged si engine. In *Annual conference on industrial electronics IECON*, pages 325–330, 2006.

[14] Paul Moraal and Ilya Kolmanovsky. Turbocharger modeling for automotive control applications. *SAE*, (1999-01-0908), March 1999.

[15] M. Mueller. Mean value modeling of turbocharged spark ignition engines. Master's thesis, DTU, 1997.

[16] Martin Muller, Elbert Hendricks, and Spencer C. Sorenson. Mean value modelling of turbocharged spark ignition engines. *SAE technical paper*, pages 125–145, 1998.

[17] S.A. Nelson, Z.S. Filipi, and D.N. Assanis. The use of neural networks for matching compressors with diesel engines. In *Spring technical conference*, volume ICE-26-3, pages 35–42, 1996.

[18] H.C. Watson, E.E. Milkins, K. Roberts, and W. Bryce. Turbocharging for fuel efficiency. *SAE*, (830014), February 1983.